Referee comment: Development and characterization of the Portable Ice Nucleation Chamber 2 (PINCii), Castarède et al., 2023

The manuscript presents a new instrument to measure ice-nucleating particle concentrations, both in the laboratory and the field. Even though there is already a high number of instruments of the same type, PINCii is a further improvement of the measurement technique. Furthermore, the authors discuss a new approach to analyze the data of a CFDC. To validate the instrument, multiple experiments including deliquescence, homogeneous freezing and heterogeneous freezing were performed and the results are compared to literature values from different studies.

Overall, the manuscript is well written and structured and gives detailed explanations of the work that has been done. However, there are some points, listed below, that would further improve the quality of the paper. My comments are structured in first more general comments and second minor comments.

Response: We thank the referee for their useful comments which helped improve the manuscript. We include our responses below, in the context of individual comments.

General comments

- Given the length of the text, there is a quite high number of figures, such as e.g. in section 2.4. I would recommend to reduce the number of figures and instead explain the outcome of the measurements in more detail in the text. The figures can then be either deleted or moved to the appendix.

Response: We understand the reviewer's comment and we combined Figures 3 and 4 into one figure. We attach the updated figure at the end of this document. We believe that the rest of the figures are necessary to the manuscript, and we would like to keep them in the main text.

- Figure 8, 9 and A1 are very complex and hard to understand. They should be simplified to a 2D plot, with AF as a color scale. If the change in AF is the important parameter for defining the onset, then the color code can also be presented as Δ AF.

Response: We understand that the 3D plots are quite complex and hard to interpret. Since this issue was brought up by two reviewers, we decided to modify Figures 8, 9 and A1 to 2D plots. We attach the updated figures at the end of this document.

- How much does a potential underestimation of the number of ice crystals due to the binning of the OPC and the set ice threshold contribute to the total uncertainty of the INP concentration? The authors provide a calculation of the ice crystal growth, however, this assumes a spherical ice crystal and a constant mass accommodation coefficient of 0.3. Based on this calculation, the threshold for ice crystal detection in the OPC was set. However, since the binning of the OPC is quite broad, some particles might not be counted as ice (or droplets), because they are not detected in the respective channel of the OPC. This could be especially relevant when measuring INPs in low concentrations.

Response: Thank you for your comment. We first want to clarify that the ice crystal growth calculations were made retroactively to ensure that our observations are aligned with theoretical expectations, and not to set the threshold for ice crystal detection in the OPC. The choice of both detector and cut-off size should be determined based on the experimental parameters.

Concerning the potential underestimation of the number of ice crystals detected, there is no single uncertainty that can be quoted in this case. We believe that when the chamber is operated to capture clear ice nucleation onsets, the uncertainties are likely small or negligible compared to the natural variability of the INP concentrations (for ambient measurements). The ability to change the ice crystal size detection threshold allows us to avoid undercounting ice crystals because the detection threshold can be chosen as a smaller (or larger) size to account for the slower (or faster) growth of the ice crystals depending on operating temperature(s). Figure A3 suggests that at -21 °C, an ice crystal grows to 5 µm in diameter at RH_i = 104 % within the 15 s residence time of PINCii. This implies that, at -21 °C, using a 5 µm detection threshold will not yield any reported INPs for RH_i < 104 %. However, this is not of concern because INPs do not freeze at such low RH for this temperature range where immersion freezing would dominate, and RHw would need to be at 100 % or higher, thus far exceeding 104 % RH_i. In theory, one could define that PINCii is not suited for measurements at RH_i < 104 % for -21 °C, i.e. that a limit of operation can be defined rather than an uncertainty. But this will not affect the applicability of PINCii since immersion freezing at RH_i =104 % would be thermodynamically impossible.

Similarly, for colder temperatures, the threshold can be reduced to 3 µm. For instance, from Fig. A3 at -31 °C and RH_i = 104 %, an ice crystal grows to 3 µm. Here again, any ice nucleation occurring at RH_i < 104 % would not be detected. As such a limit of operation can be defined but also immersion freezing would RH_i >>104 % and thus would not be of concern. One could argue that already at 105 % at -35 °C, deposition nucleation is reported (Welti et al., 2009 ACP). In this case, an interference from liquid droplets is not a concern, so the ice detection threshold can be further decreased to 2 µm or even 1 µm if the aerosol being sampled is below 800 nm in diameter so as to not interfere with the 1 µm OPC channel.

Therefore, the flexibility in choosing the ice threshold is key to avoid undercounting ice crystals. Moreover, in the absence of such flexibility, one can define a RH range limit of operation such as: above RHi >104 % and below water droplet breakthrough.

In theory, this exercise is also dependent on the aerosol particle size being sampled. If super micron particles are being sampled in the field, one has to define the ice threshold as that above the largest sampled unactivated aerosol signal in the OPC. And a choice in the ice crystal threshold size can always be customized to avoid undercounting and to define a limit of operation. So the colder temperature measurements can even use a size threshold of 1 µm as long as the sampled aerosol sizes are below 500-800 nm and are not detected in the optical 1 µm channel.

We also note that the calculations in Figure A3 assume spherical ice crystals and compact spheres. However, this is not a poor assumption for detection sizes of below 5 µm as non-spherical features at such small sizes are hard to detect or quantify. Moreover, even in depolarization detectors, crystals of this size appear highly spherical (Mahrt et al., 2019 AMT).

Minor comments

- L6: The phrase “very low concentrations” should be supported with numbers of the range of the limit of detection

Response: We agree with the reviewers, and we have rephrased the sentence to add some numbers:

“Notably, a specific icing procedure results in low background particle counts, which demonstrates the potential for PINCii to measure INPs at low concentrations (< 10 #/L).”

- L21-22: In line 21 you are writing “heterogeneous nucleation”, however, in the following sentence in L22 you call it “heterogeneous ice nucleation”. You should stick to one term, preferably the second one.

Response: We agree, and we changed to “heterogeneous ice nucleation”.

- L39: Mention that the CFDC-IAS has a cylindrical shape

Response: We thank the reviewer for this suggestion. We added a mention to the shape of the CFDC-IAS L39:

“[...] the cylindrical CFDC-IAS (Handix Scientific, Boulder, Colorado, USA) [...]’

- Figure 1: A list inside the figure explaining the letters (a) to (k) would help for an easier understanding. The color of (f) (refrigerant cooling coil pipes) should be changed, because it is difficult to differentiate it from the other items.

Response: As the figure is already quite full, we believe that adding text next to it would make it harder to read. Moreover, the annotations are explained in the caption located directly under the figure. Considering this and the fact that the figure was optimized for the one-column format, we would rather keep the figure as is. We agree with the reviewer that the color of the cooling pipes was difficult to see, and we changed the color as suggested (see updated figure at the end of this document).

- L89: Briefly explain what ETH-IODE is and what it is used for

Response: We propose to rephrase the sentence at L89 to:

“[...] designed for mounting the Ice Optical DEpolarization detector (IODE; Nicolet et al. 2010) used to distinguish between water droplets and ice crystals.”

- L101: Explain the abbreviation R23

Response: R-23 is the official product name of this refrigerant and is not necessarily an abbreviation. Nonetheless, we propose rephrasing L101 to clarify:

“[...] cold injection points given that the refrigerant R-23 (trifluoromethane) operates with [...]”

- L117: How much longer is the main chamber of PINCii compared to other CFDCs? You should give at least a range of numbers

Response: Thank you for this suggestion. We rephrased L117 to indicate the chamber lengths:

“[...] PINCii has an elongated design, where the main chamber (100 cm) and the evaporation section (43 cm) are longer than in other instruments (e.g. PINC and SPIN have main chambers of 56.8 and 100 cm, and evaporation sections of 23 and 25 cm respectively).”

- Figure 5: The symbols of the first and second experiment are very hard to distinguish in the plot. As it is written in the text, the data are presented as normalized values, so it might not be needed to present them in different symbols. If the authors think, that it gives the reader some value to know which data points were recorded on which day, they should divide the figure in two sub plots. It might be also beneficial to mark the range in which the data points represent either an activated cloud droplet or an ice crystal.

Response: In Figure 5 we want to show that the data points overlap since it means that the results are identical for both experiments (after normalization) even though they were done on two separate days; thus, making them distinguishable is not our objective. However, since there were indeed two experiments on two different days, we do want to present the data with different symbols.

The experiments presented in Figure 5 were conducted with a temperature gradient along the evaporation section (so the evaporation section does not evaporate anymore). Thus, we cannot distinguish activated cloud droplets from ice crystals. We modified the text to make it more clear:

L167 "In this work, we use this feature to show that the chamber can actively grow droplets."

And added a sentence L169:

"First, we study the activation of polydisperse ambient aerosol particles, and then we present a deliquescence experiment with 200 nm Sodium Chloride (NaCl) particles. For both experiment types, the temperature gradient along the main chamber is extended to the evaporation section, so the evaporation section is no longer evaporating droplets."

- L234-239: The authors should elaborate a bit more the outcome of figure 8(a) by giving numbers e.g. at which RH_lam activation happens for different temperatures and how much it differs from the Koop line.

Response: We added more information L234-239 and we hope that changing figure 8 to 2D plots will also improve clarity.

"Presenting data in this way shows an increasing deviation from the Koop et al. (2000b) curve towards lower $RH_{i,lam}$ as the temperature increases from T_{lam} = -45 °C, with the maximum deviation at T_{lam} =~-40 °C where the freezing onset is observed 7.2 % $RH_{i,lam}$ below the Koop et al. (2000b) curve. Figure 8a also shows a slight deviation from the Koop et al. (2000b) curve at T_{lam} = -49 °C, where the freezing onset is observed 1.7 % $RH_{i,lam}$ above the Koop et al. (2000b) curve. [...]"

- L247-248: How is it seen that some ice crystals did not grow to 5μm. I guess it can be seen by the ice threshold that is shifting to a lower RH_lam from Fig. 8(a) to 8(b). However, a short note on that might be helpful for the reader.

Response: Yes indeed, it is seen by the ice nucleation onset that is shifting towards lower $RH_{i,lam}$. We added a note L247-248 to be more clear:

"Although the change in the size threshold does not affect the activation curves for T_{lam} > -45 °C, the ice nucleation onsets shift towards lower $RH_{i,lam}$ for Tlam < -48 ◦C, illustrating the existence of activated crystals that have not grown fully to 5 μm for these temperatures. "

- L274-276: Replace one of the "significantly"

Response: The "significantly" L276 was changed to "substantially".

- Figure 9: In the caption, replace "triangles" by "squares"

Response: Thank you for spotting this mistake, we changed it to "squares".

- L329: Add a short note why the rapid cooling should be avoided

Response: We rephrased L329 to add more information:

"To avoid cooling too rapidly, which would deteriorate the quality of the ice-coating and lead to high background counts, the setpoint temperatures are changed [...]"

- L337: "exceptionally" and "mediocre" need to be defined in terms of values

Response: The values are given a few lines later (L341-343). The sentence L337 merely introduces Figure 10.

- L341: Remove "exceptionally"

Response: We removed "exceptionally" as suggested (also L337).

- L343: A short discussion about the background concentration after 3 ramps is missing

Response: We propose to add some information L343:

"However, after three $RH_{i,lam}$ ramps, the ice layer clearly deteriorated and the median background count is 60.0 #/L, which is too high for continuing with the measurements."

- Figure 11: Was the droplet break through only measured for four of the scans?

Response: Yes, as presented in Figure 7, droplet breakthrough was measured for four temperatures (-20, -25, -30 and -35 °C).

- L465: Rephrase to "sampling from sources with INP concentrations as low as …"

Response: We rephrased as suggested:

"This means that PINCii is suited for sampling low INP concentrations (< 10 #/L)."

- Figure A1: This figure is mentioned quite often in the text. Therefore, I suggest to move it from the appendix to the main text.

Response: Figure A1 is mentioned only twice in the text (L272 and L415) and therefore we would like to keep it in the appendix. There is however the issue that both the first figure and the first section of the appendix have the same name (A1), which might be confusing when mentioning one or the other. This is a typesetting issue which we expect will be dealt with in the case of acceptance.

Updated figures:

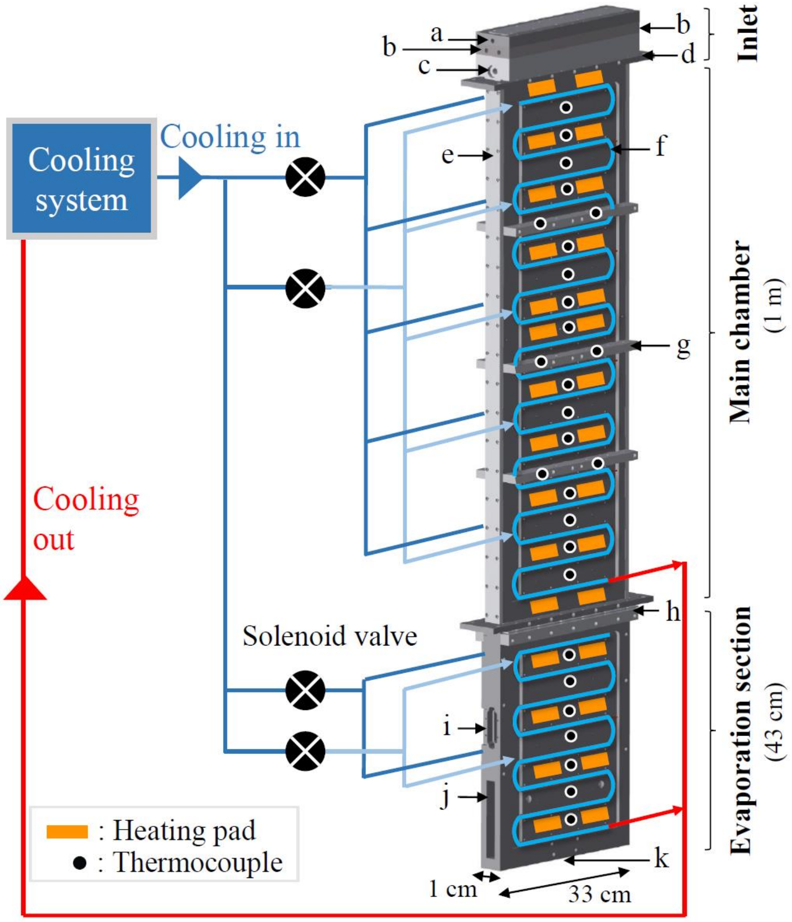

Figure 1. Schematic of PINCii and its cooling system, including the main elements of the chamber: (a) the sample inlet, (b) the sheath flow inlets, (c) the water level sensor port, (d), (e) and (h) the SustaPEEK flanges thermally isolating sections of the chamber, (f) refrigerant cooling coil pipes, (g) support bars, (i) window port, (j) the lower evaporation section with material removed, and (k) the exit hole. The location of the coolant injections, heating pads and thermocouples on a single wall are also depicted. The injection of coolant to the different chamber sections is controlled independently, while multiple thin capillaries located after the solenoid valves distribute the coolant evenly to the selected section.

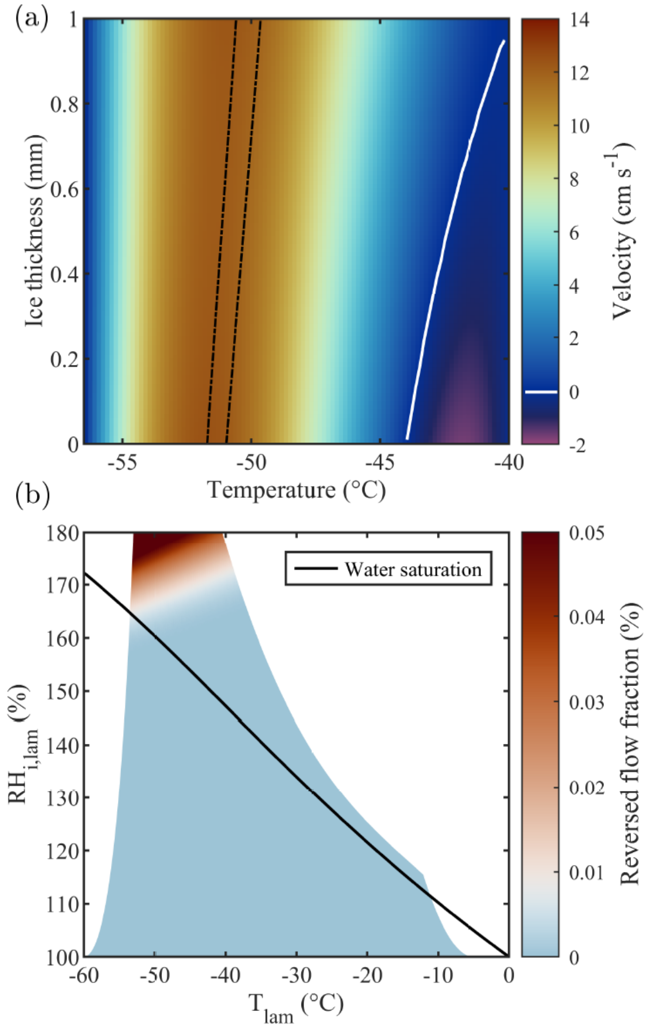

Figure 3. (a) Flow velocity as a function of ice thickness for fixed wall temperatures of -40.0 and -56.5 °C, chosen to represent homogeneous freezing conditions PINCii's main chamber. These conditions (T_{lam} = -51.3 °C and $RH_{i,lam}$ = 155.7 % at ice thickness = 0 mm, and T_{lam} = -50.1 °C and $RH_{i,lam}$ = 154.7 % at ice thickness = 1 mm) are representative of extreme chamber operations for PINCii, with the greatest potential for buoyancy effects. The lamina position is depicted by the dashed black lines. The white contour line corresponds to a velocity of 0 cm/s and emphasizes where the region with negative velocity starts. (b) Achievable T_{lam} and $RH_{i,lam}$ assuming fixed wall temperatures between -5 and -60 °C and accounting for the droplet breakthrough results presented in section 3.1. The color map represents the reversed flow fraction defined as the ratio between the reverse (upward) flow and the normal (downward) flow in the chamber, assuming a 1 mm ice layer on each wall. The black solid line represents water saturation ($RH_{liq,lam}$=100 %).

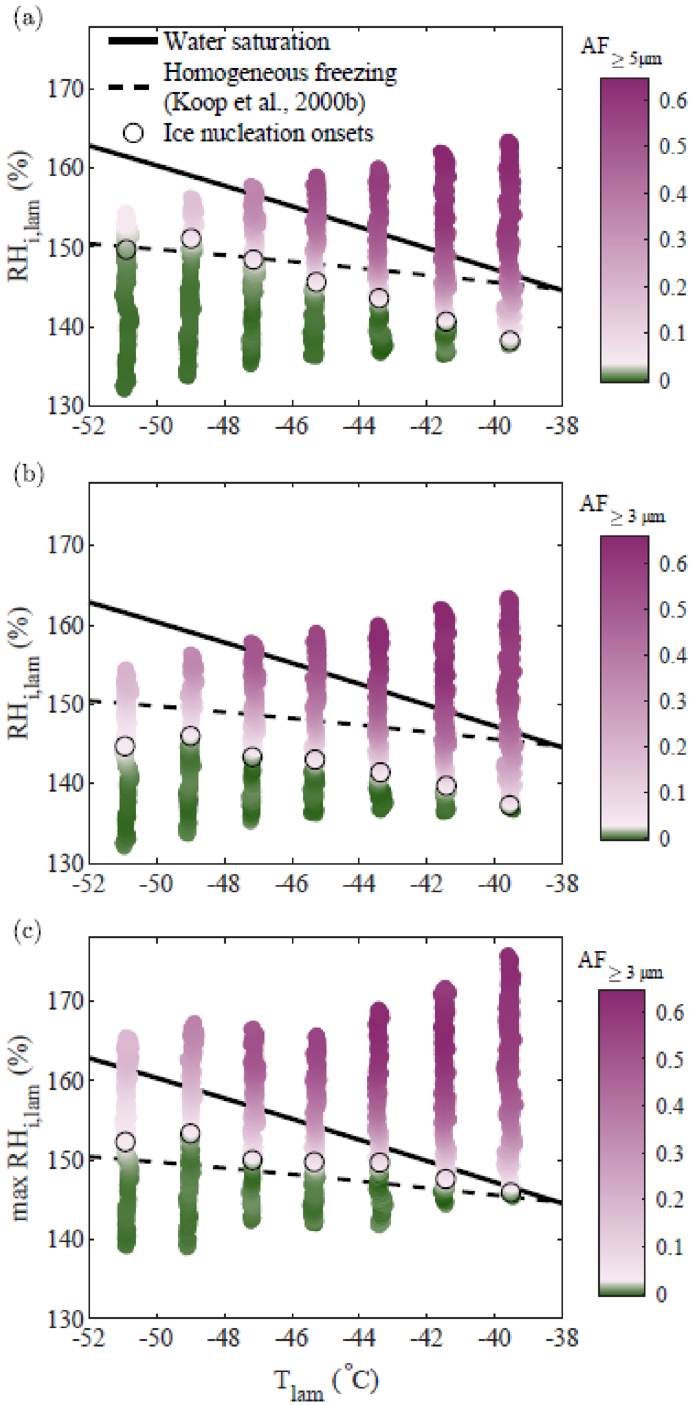

Figure 8. Homogeneous freezing of 200 nm NaCl particles plotted as a function of T_{lam} and $RH_{i,lam}$ represented in three different manners: (a) AF of aerosols with dp ≥ 5 µm plotted as a function of the average Tlam and RHi,lam. (b) AF of aerosols with dp ≥ 3 µm plotted as a function of the average T_{lam} and $RH_{i,lam}$. (c) AF of aerosols with dp ≥ 3 µm plotted as a function of the average T_{lam} and the maximum $RH_{i,lam}$. The theoretical curves for water saturation (solid black line) and homogeneous freezing (dashed black line, calculated with Δaw = 0.2946 following Koop et al., 2000b) were added for supplementary information. In each plot, the color scale is used to represent changes in the AF. The white region in the color bars represents the ice nucleation onset, which was estimated using the median of the inflection points obtained for each activation curve (see A1 for more information).

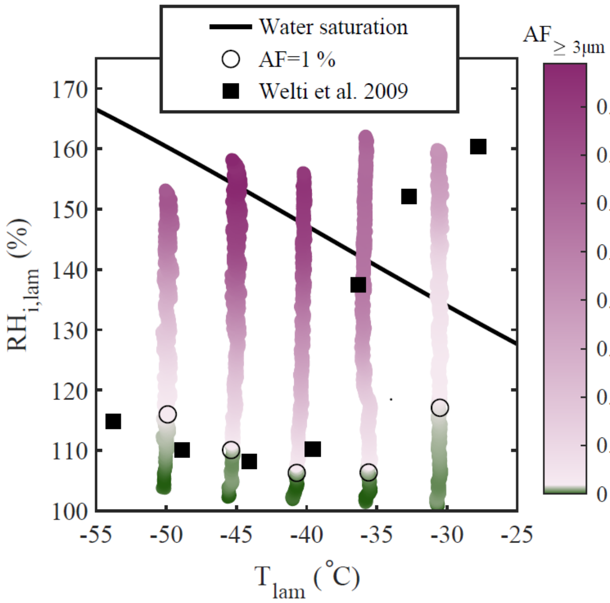

Figure 9. Heterogeneous freezing of size-selected 200 nm NX-illite particles. The AF of aerosols with dp ≥ 3 µm is plotted as a function of the average T_{lam} and $RH_{i,lam}$. The white region in the color bars represents AF=1 %. The AF=1% is also plotted as circles for comparison with the AF=1 % onset of similar particles reported in Welti et al. (2009), shown here as black squares.

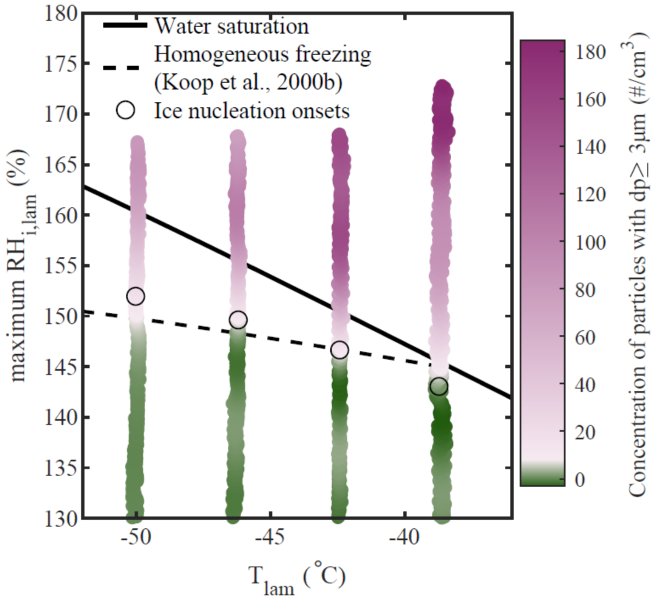

Figure A1. Homogeneous freezing of 200 nm particles generated from a natural salt sample collected in the Qaidam basin, China. Note that, due to an instrumental malfunction, the CPC was not running and thus the AF could not be calculated for this experiment. The concentration of aerosols with dp ≥ 3 µm is plotted as a function of the average T_{lam} and the maximum $RH_{i,lam}$, and the color scale is used to represent changes in the concentration. The white region in the color bars represents the ice nucleation onset which was estimated using the median of the inflection points obtained for each activation curve (see A1 for more information). The theoretical curves for water saturation (solid black line) and homogeneous freezing (dashed black line, calculated with Δaw = 0.2946 following Koop et al., 2000b) were added for supplementary information.